

Stability Evaluation of the Flight Trajectory of Unmanned Aerial Vehicle in the Presence of Strong Wind

Lucjan Setlak, and Rafał Kowalik
Aviation Division, Department of Avionics and Control Systems
Polish Air Force University
ul. Dywizjonu 303 no. 35 Deblin 08-521,
Poland
l.setlak@law.mil.pl, r.kowalik@law.mil.pl

Abstract: - The article presents the results of simulation tests assessing the movement dynamics of unmanned aerial vehicle in difficult atmospheric conditions, which is a very strong wind exceeding 120 [km/h]. The results obtained at the simulation research stage were presented in the form of flight trajectory waveforms and changes occurring due to the strong wind. All obtained results were performed for two assumptions, namely windless and windy conditions. The wind strength in the analyzed system was treated as a disturbance of the UAV dynamics, which affected the change of the speed parameter and its position in the atmospheric space, as a **consequence** of which the flight stability was disturbed. Taking the above into consideration, it was assumed in the research that the obtained results should be carried out in a dynamic manner in order to realize the momentary dynamics of the motion of the tested flying object. The obtained results confirm that if we have accurate slip and angle of attack measurements for UAV, using electronic sensors we can correctly determine the value of the wind speed and the trajectory of the flight. The entire process can be carried out independently of the type of regulators used in the unmanned aerial vehicle control system. The article also presents an overview of other adverse physical phenomena occurring in the atmosphere, having an adverse effect on the UAV flight stability. In the final part of this article, based on simulation studies, the obtained test results were analyzed and practical conclusions were formulated.

Key-Words: - evaluation, stability, flight trajectory, unmanned aerial vehicle

1 Introduction

Currently, unmanned flying machines, including UAV (*Unmanned Aerial Vehicle*) remotely controlled and radio-controlled by the operator are commonly used. They are already used not only in various industrial sectors (aviation, car industry, shipbuilding, etc.), but also constitute an increasingly popular branch of modeling, including the hobby type [1], [2], [3].

It should be noted that the synthesis of a control system for a quadcopter is not a trivial task, among others, due to the non-linear nature of the dynamics of this object and its structural instability. In view of the above, working only with the physical model of a quadcopter can result in potential material damage resulting both from damage to the device and from elements in its immediate vicinity. Therefore, it is advisable to develop a model that allows safe pre-analysis of the solutions being developed.

In addition, due to the growing interest in various quadcopter solutions, it is expected that the proposed model will not only improve the operation of the constructed structures, but most of all it will

find practical applications. The description of the approach to modeling the dynamics of quadcopter and the identification of its parameters can be found in many publications, including [4], [5].

This article presents a methodology that allows not only for the construction of a practical mathematical model of a quadcopter, including its structure and parameters, but also taking into account executive systems. Therefore, the key achievements of this work with reference to e.g. [6] is the use of an alternative abstraction of the quadcopter object and system, and the inclusion of a drop in the supply voltage in the mathematical model. Thanks to this approach, it is possible to design control systems with compensation for the effects of voltage drop.

The above solution translates into lowering the uncertainty in the functioning of the control system, which in turn improves the quality of the control process. It is also worth adding that this type of solution is not currently widely used in modeling. Based on the above considerations, collected data and knowledge in the field of UAV construction, this work based on the review of existing solutions

and created mathematical models and selected computer simulations, served to analyze the impact of atmospheric conditions on the waveform of radio and satellite waves. In addition, selected simulation tests were carried out, and above all performing the quadcopter flight in windy and windless conditions, and recorded flight parameters were used to determine the effect of wind on the spatial position of the quadcopter [7], [8].

2 Unfavourable Atmospheric Conditions Affecting the Propagation of Radio Waves

As previously mentioned, the entire Unmanned Aircraft (UAV) control process is based on the use of radio waves transmitted from the transmitters of control equipment to receivers located on the UAV and back. Physical phenomena occurring in the atmosphere of the Earth exert a key influence on the propagation of radio waves, and what is related to the performance of UAV flights.

The phenomena that have an impact on the propagation of radio waves include, among others:

- refraction,
- diffraction,
- tropospheric dispersion,
- rainfall,
- atmospheric gases,
- clouds and fogs,
- scintillations,
- polarizing interferences.

2.1 Refraction

Refraction is an atmospheric phenomenon, during which the radio wave collapses, resulting from inhomogeneous atmosphere structure. According to *Snellius'* law, every electromagnetic wave breaks down during the transition from one center to another, characterized by a different refractive coefficient.

The instability of the refractive coefficient causes the trajectories of electromagnetic waves in the atmosphere to be curved. Due to the fact that the value of refractive coefficient n slightly exceeds 1, the use of another parameter, namely the refractive coefficient N , determined using the following relationship, was assumed:

$$N = (n - 1) \times 10^6 \quad (1)$$

where:

N - refractive coefficient,

n - the refractive coefficient of the atmosphere.

The refractive coefficient N is influenced by the temperature T , the pressure p and the atmospheric humidity e [9], [10]:

$$N = \frac{77,6}{T} \left(p + 4810 \frac{e}{T} \right) \quad (2)$$

where:

N - refractive coefficient,

T - temperature of the atmosphere,

p - atmospheric pressure,

e - humidity of the atmosphere.

As the height increases, the refractive coefficient decreases by an average of 40 units per kilometer due to the decrease in pressure and humidity. The trajectory of the radio wave takes the shape of the arc directed by the convexity towards the upper layers of the atmosphere [11], [12].

Atmospheric refraction is also determined by the severity factor of refraction K :

$$K \approx \left(1 + \frac{dN}{dh} \times \frac{1}{157} \right)^{-1} \quad (3)$$

where:

K - refractive coefficient,

dN - derivative of the refractive coefficient,

dh - derivative of heights.

As a result of the phenomenon of refraction, the trajectories of propagating radio waves are curved in the atmosphere. The most frequent deviation of radio waves towards the surface of the Earth, then the gradient of the refractive coefficient is negative. This is not a problem for receiving signals during flights.

The problem arises during unfavorable weather conditions in the form of clouds or rainfall. Then the radio wave due to the curvature of the top can never reach the receiving station (Fig. 1).

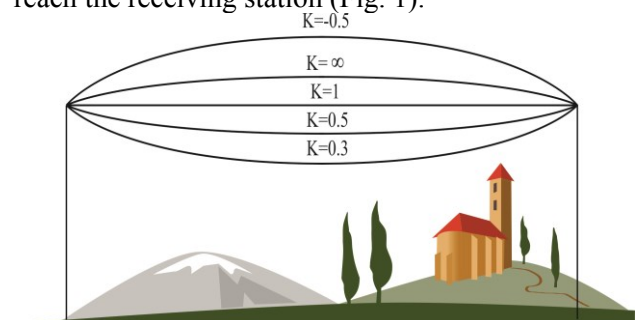


Fig. 1 Radio wave propagation at a different refractive coefficient severity K

The refractive indicator gradient rarely has a constant value, which in turn contributes to the propagation of radio waves across different curves. This leads to multi-directional propagation and the scattering of radio waves in the atmosphere. Due to

the occurrence of both these phenomena, deep disappearances may occur in the receiving antenna, and in specific conditions, atmospheric vents may form.

On the one hand, atmospheric ducts enable the propagation of radio waves over long distances; on the other hand such extensive propagation of radio waves increases the probability of distortions of distant radio-communication systems [13], as illustrated in the figure below (Fig. 2).

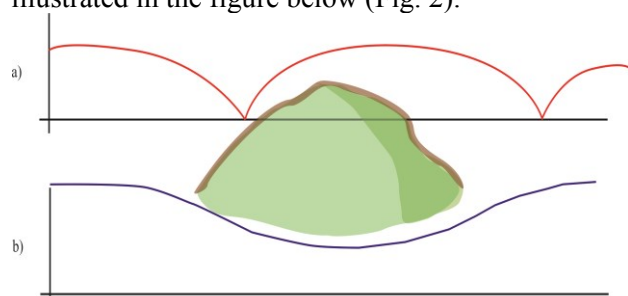


Fig. 2 Atmospheric ducts: a) - ground level, b) - elevated

2.2 Diffraction

Diffraction has a twofold effect on UAV controllability. Skilful use of it allows you to fly long distances, but not to adapt to the specifics of this phenomenon makes it impossible to perform a safe flight.

The diffraction pattern is defined as the deflection of an obstacle wave with dimensions larger or comparable to the wavelength, which applies to each wave type. When considering the phenomenon of diffraction, the *Huygens'* principle is used, according to which all points of the wave front can be treated as the source of new spherical waves [14], which was depicted in the next figure (Fig. 3).

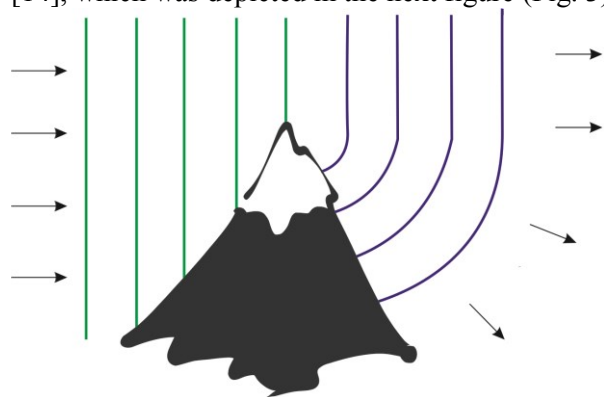


Fig. 3 The diffraction phenomenon at an obstacle

In order to change the negative effect of the diffraction phenomenon on radio waves, one should take care of the lack of obstacles in the area of the first antenna when designing radio systems. It may

be an area around the terrestrial antenna sending UAV control signals. The diffraction phenomenon is most often used in off-horizon radio lines [15], [16].

2.3 Tropospheric dispersion

The continuous movement of the atmosphere of the Earth is greatly affected by its uneven heating by the sun's rays and the exchange of heat between the surface of the Earth and the layers of the atmosphere of the Earth. Near the surface of the Earth, where air movements are most intense, areas with variable refractive indicator arise.

While the radio wave during its course hits an area with a refractive indicator that differs from the refractive indicator of the surrounding air, it is dispersed. As a result, part of the energy of the radio wave disperses, while the larger part of it passes through this area without changing the direction, while the remaining part is reflected back towards the Earth, thanks to which it has the ability to reach the receiving antenna.

The negative side of tropospheric dispersion that makes flight difficult with UAV is the attenuation of the radio wave due to its dispersion in the troposphere. The attenuation of the radio wave reaches the highest value when using small angles of elevation of the ground station antenna, however, it does not exceed 3 [dB] (Fig. 4).

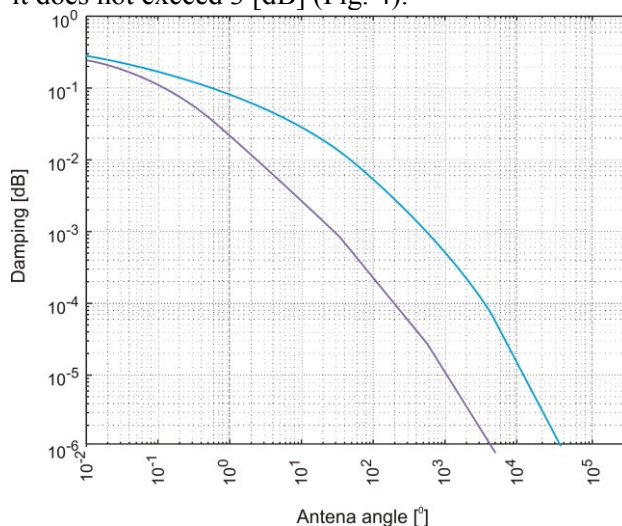


Fig. 4 The value of attenuation resulting from the scattering of the radio wave (A) and the standard deviation (B) depending on the elevation angle of the earth station in connection with the geostationary satellite [17]

The phenomenon of tropospheric scattering is most often used in amateur communication and off-horizon radio lines. To limit the value of the scattering angle and minimize it, the smallest

antenna angle kits as well as half-power antenna angles are used, with the upper limit being the angle of $1,7^{\circ}$ [18].

2.4 Rainfall

In the case of precipitation, you can not talk about any positive aspect that affects the maneuvering of the UAV. The mere fact that raindrops could get inside the drone and damage its equipment, while snowfall could freeze the surface of the controls and immobilize them, leaves no doubt that it is better not to perform any UAV operations during such atmospheric phenomena [19], [20], [21].

In addition to the aforementioned factors, the occurrence of radio wave damping due to rainfall is also significant (Fig. 5). This attenuation increases in value if:

- precipitation is intense,
- precipitation occurs on a significant part of the radio route segment,
- higher frequency of the radio wave is used.

On the basis of the ITU-R (*International Telecommunication Union - Radiocommunication Sector*) telecommunications sector, the dependence of radio wave suppression on rainfall was determined. This dependence can be determined using the following formula:

$$A_p = \gamma_R \times d \times r \quad (4)$$

where:

A_p - suppression exceeded by „p” percent on an annual basis [dB],

γ_R - unit attenuation [dB/km],

d - section of the radio route on which rainfall may occur [km],

r - route reduction coefficient.

2.5 Clouds and fogs

Clouds and fogs arise from the phenomenon of condensation of water vapor in the atmosphere of the Earth. Depending on the type and level of occurrence, they are composed of water droplets, ice crystals or a combination of both. Mists arise and occupy the mundane atmosphere layer, while clouds can form up to a height of up to several kilometers.

Attenuation by clouds and fogs is similar to the attenuation of radio waves during precipitation. It increases as the cloudiness increases and the density of fog increases. The cloudier a significant portion of the radio wave route is, the more likely it is that the signal will spread from the clouds towards the earth. During the occurrence of the above phenomena, no flights are also made due to visibility restrictions [22], [23].

3 Simulation and Course of Research

In order for the quadcopter to provide the necessary data, the flight would have to last at least 70 km/h. In the place where the test was carried out, the profile of wind at medium altitudes is not turbulent, especially in the case of southern winds.

The flight parameters were estimated using the equations presented in the above subsection with the exception of the *Euler's* angles, whereby these angles are calculated by flight controllers [24], [25].

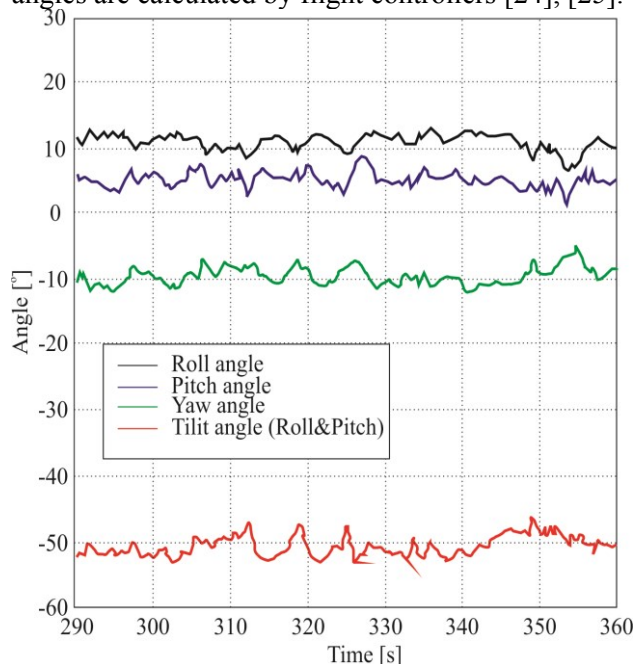


Fig. 5 UAV angular position during flight generated by the on-board controller

The graph above (Fig. 5) shows the angles achieved by the quadcopter during flight operations [26], [27], [28], [29].

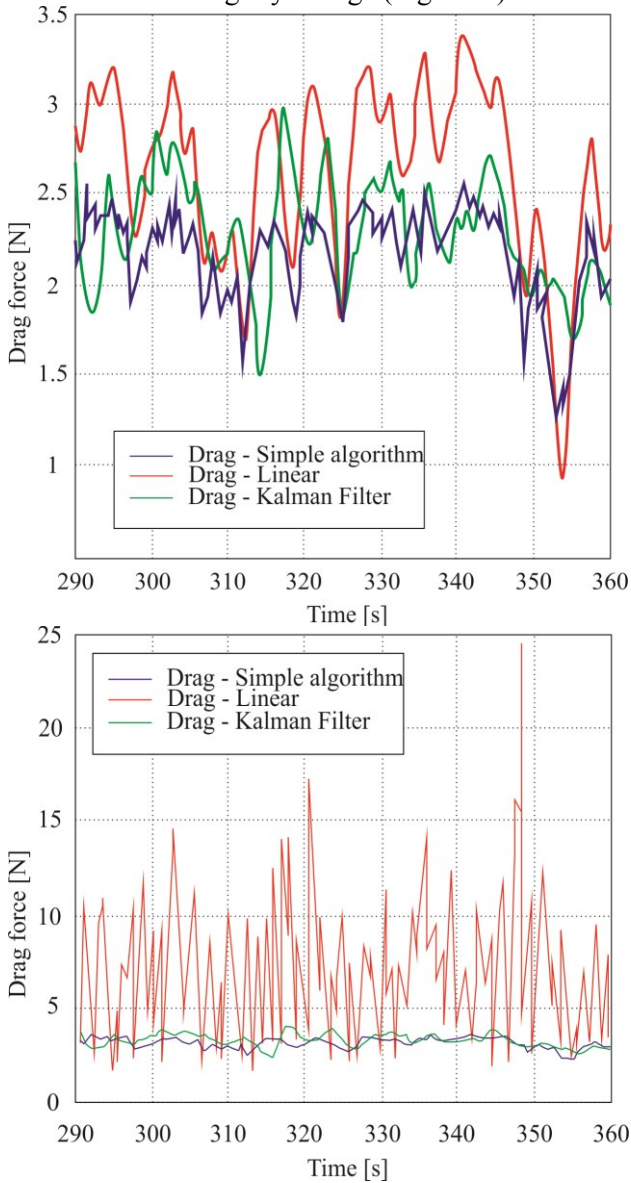
Table 1 Profile parameters measured by the meteorological device

| Parameter | Mean | Maximum | Minimum | Standard deviation |
|--------------------|------|---------|---------|--------------------|
| Wind speed [m/s] | 4.6 | 6.2 | 2.6 | 0.8 |
| Wind direction [°] | 187 | 228 | 151 | 1.2 |

The table above (Table 1) presents the minimum, average and maximum values of wind direction and its speed during aerial maneuvers. The wind direction was measured from the magnetic north.

The values of these angles are used to calculate the resistance force affecting the drone. Using the method in which linear equations occur for calculations, take into account the originating noise

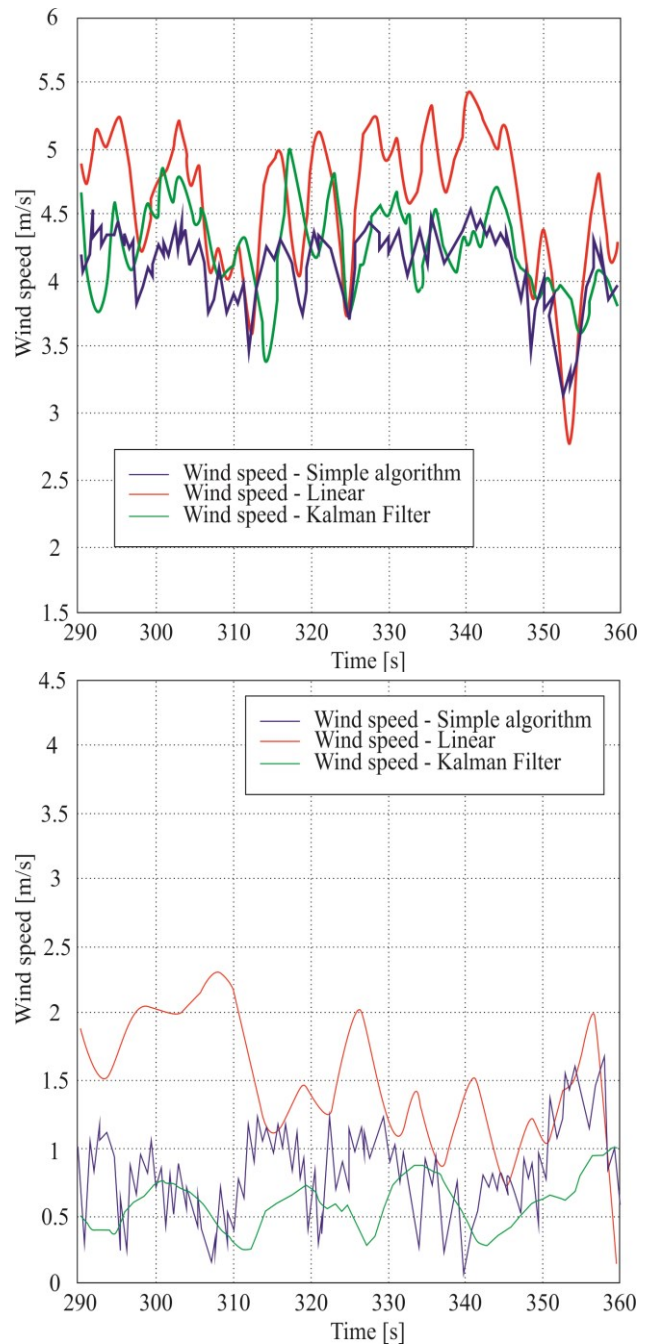
from accelerometers which, as expected, have a huge impact on the results of calculations. If the method with the *Kalman* filter is used, the answers obtained would slightly change (Figs. 6-7).



Figs. 6-7 Estimation of the resistance force - the data from the accelerometer passes through the filter

The average resistance value can be obtained by using each of the three methods.

After receiving all the averaged values, the equation can be calculated, and the results obtained after calculating the wind direction and velocity are presented in the following graphs (Figs. 8-9).



Figs. 8-9 Estimation of wind speed

In order to broaden and compare the scope of tests, the flight was also performed in windless conditions in the same place.

The measurement lasted 25 seconds. The results of the drone reaction are shown in the following figures (Figures 10-11).

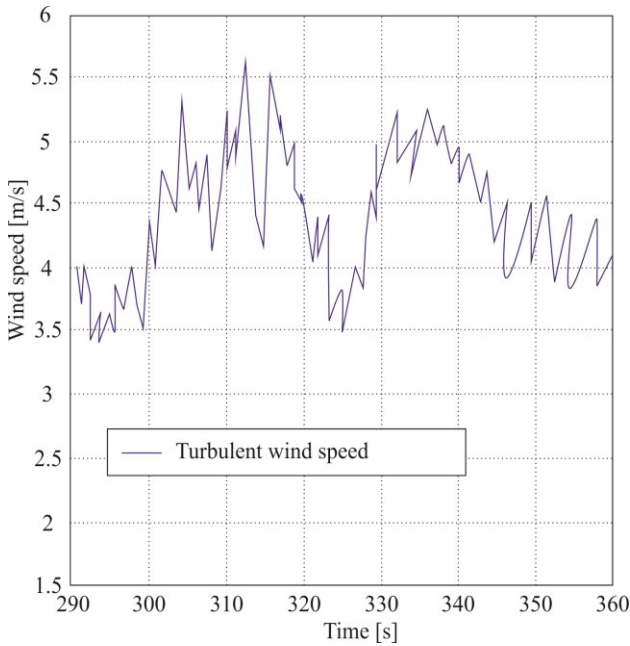


Fig. 10 Estimation of wind speed in windless conditions

Due to the wind effect, close to zero, erroneous estimates were generated despite expectations. Analyzing the above drawings, it was found that the calculated wind velocities partially coincide with the data obtained and the anemometer.

UAV self-tilting was also observed during incoming air streams, as evidenced by the results related to the wind direction. Therefore, the actions taken to calculate the direction of this atmospheric phenomenon were correct.

The following table (Table 2) compares statistics on wind profile estimation with data received from the anemometer.

Table 2 Statistics for wind profile estimation

| | Wine speed | | Wind Direction | |
|------------------|------------|--------------------|----------------|--------------------|
| | Mean [m/s] | Standard deviation | Mean [°] | Standard deviation |
| Anemometer | 4.6 | 0.8 | 187 | 1.2 |
| Simple algorithm | 4.287 | 0.264 | 195 | 7.07 |
| Linear equations | 4.71 | 0.477 | 195 | 7.07 |
| Kalman filter | 4.41 | 0.297 | 195 | 7.07 |

Analyzing the above table, it was noticed that the average values of wind speed and its direction are comparable, and standard deviations are not noticeable. Time intervals for the anemometer and

drone differ in values, which prove the receivables to take into account comparative conclusions. A bad estimate of the profile is caused by the instability of the quadrocopter as a result of the wind.

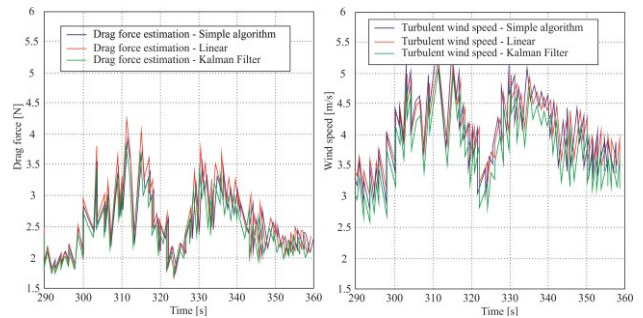


Fig. 11 Turbulent wind profile

In connection with the above, the current platform will only work with well-defined wind profiles. All three tests carried out give good results in the course of continuous winds, however, the actual wind profile is not constant, and even a turbulent flow occurs. Using the *Bladed* program, the methods for the turbulent profile along the X axis was checked (Fig. 12).

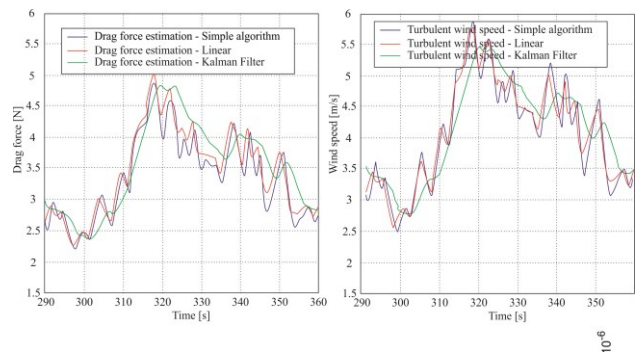


Fig. 12 The strength of resistance and wind speed along the X axis

By comparing the above graphs, it can be concluded that all three methods show some similarity. To distinguish them one should carefully analyze the obtained graphs (Fig. 13).

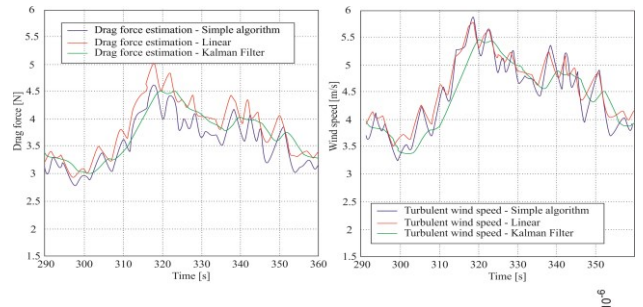


Fig. 13 The waveform of the simulation process detailing the data defining the resistance and wind speed along the X axis

When changing the UAV flight dynamics based on the straight line method and linear equations, you can not accurately determine the wind speed. The method that gives a very accurate result is a method using the *Kalman* filter. It applies when using real data and due to the fact that there is noise during the measurements, especially taking into account the data from the accelerometers. The use of the *Kalman* filter takes into account the phenomenon of noise and provides a more accurate answer.

4 Conclusions

On the basis of the presented work, it was determined that atmospheric phenomena are not indifferent for each aircraft (airplane, helicopter). In the case of unmanned aerial vehicle in the event of failure due to rain or tropospheric dispersion, the situation does not seem to be frightening, because the UAV operator is safely on the ground and can safely try to restore the drone's flight. The situation is different in the case of aircraft in which the pilot is at the controls and in case of exposure to negative atmospheric phenomena he must control the aircraft and save his own life and passengers.

Based on the analysis of unfavorable atmospheric conditions for propagation of radio waves, it can be noticed that the impact on the controllability of the UAV are not only those atmospheric phenomena that are responsible for the correct or otherwise opposite waveform of a radio wave, but also a phenomenon such as wind, having a direct impact on the spatial position of the drone. Such phenomena should not be underestimated, while performing air operations should be carried out with high accuracy and awareness of the existence of unfavorable factors.

Due to the constantly evolving technique in the field of UAV and more and more innovative pieces of equipment [30], [31], you can be sure that in the near future there may be devices neutralizing the impact of adverse weather conditions, and flights to the farthest corners of the world will not be an obstacle even for an amateur with adequate financial background.

References:

[1] Lee, B., Park, P., Kim, K., Kwon, S., *The Flight Test and Power Simulations of an UAV Powered by Solar Cells, a Fuel Cell and Batteries*, J. of Mechanical Science and Technology, 28 (2014), pp. 399-405.

[2] Setlak, L., Kowalik, R., and Redo, W., *Study of multi-pulse rectifiers of the PES system in*

accordance with the concept of a more electric aircraft, WSEAS Transactions on Systems and Control, Volume 13, 2018.

- [3] Allen, M., and Lin, V., *Guidance and Control of an Autonomous Soaring UAV*, NASA/TM-2007-214611, 2007.
- [4] Langelaan, J.W., Alley, N., and Neidhoefer, J., *Wind Field Estimation for Small Unmanned Aerial Vehicles*, AIAA Guidance, Navigation and Control Conference, 2010.
- [5] Choi, H.S., Lee, S., Lee, J., Kim, E.T., and Shim, H., *Aircraft Longitudinal Auto-landing Guidance Law Using Time Delay Control Scheme*, Transactions of the Japan Society for Aeronautical and Space Sciences 53 (2010), pp. 207-214.
- [6] Yoon, S. and Kim, Y., *Constrained Adaptive Backstepping Controller Design for Aircraft Landing in Wind Disturbance and Actuator Stuck*, Int. J. Aeronaut. Space Sci.,13 (2012), pp. 74-89.
- [7] Osborne, J., and Rysdyk, R., *Waypoint Guidance for Small UAVs in Wind*, AIAA Infotech@Aerospace, Sep. 2005.
- [8] Ahn, S. M., Hwang, S. J., Lee, Y. G., Kim, C., *Development of Electrical Air Vehicle for Long Endurance*, Asia-Pacific Intern. Symposium on Aerospace Technology (APISAT), 2013.
- [9] Choi, H.S., Lee, S., Ryu, H., Shim, H. Ha, C., *Dynamics and Simulation of the Effects of Wind on UAVs and Airborne Wind Measurement*, Transactions of the Japan Society for Aeronautical and Space Sciences, 58 (2015), pp. 187-192.
- [10] Lee, S., Lee, J., and Lee, D.S., *Lateral and Directional SCAS Controller Design Using Multidisciplinary Optimization Program*, J. Korean Soc. Aeronaut. Space Sci.,40, 3 (2012), pp. 251-257.
- [11] Zhen, Li, Tiansheng, Hong, Ning, Wang, Tao, Wen, *Data transmission performance for 2.4 GHz in-field wireless sensor network*, Computer Engineering and Technology (ICCET) 2010 2nd International Conference on, vol. 1, pp. V1-465-V1-469, 2010.
- [12] Hwang, S., Kim, S., Kim, C., Lee, and Y.G., *Aerodynamic Design of the Solar-Powered High Altitude Long Endurance (HALE) Unmanned Aerial Vehicle (UAV)*, 17 (2016), IJASS, pp. 132-138.
- [13] Kerr, D.E., *Propagation of Short Radio Waves* (1951).
- [14] Ting, Fei, Le-Wei, Li, Tat-Soon, Yeo, Hai-Long, Wang, Qun, Wu, *A Comparative Study of Radio Wave Propagation Over the Earth*

Due to a Vertical Electric Dipole, Antennas and Propagation IEEE Transactions on, vol. 55, no. 10, pp. 2723-2732, 2007.

- [15] Kroonenberg, A., Martin, T., Buschmann, M., Bange, J., and Vorsmann, P., *Measuring the Wind Vector Using the Autonomous Mini Aerial Vehicle M2AV*, Am. Meteorol. Soc., 25 (2008), pp. 1969-1982.
- [16] Setlak, L., and Kowalik, R., *The effectiveness of on-board aircraft power sources in line with the trend of a more electric aircraft*, 2018 19th International Scientific Conference on Electric Power Engineering, EPE 2018 – Proceedings.
- [17] Choi, H.S., Lee, S., Ryu, H., Shim, H. Ha, C., *Dynamics and Simulation of the Effects of Wind on UAVs and Airborne Wind Measurement*, Transactions of the Japan Society for Aeronautical and Space Sciences, 58 (2015), pp.187-192.
- [18] Colgren, R.D., Frye, M.T., Olson, W.M., *A Proposed System Architecture for Estimation of Angle-of-Attack and Sideslip Angle*, AIAA, pp. 743-750, 1999.
- [19] Wise, K.A., *Flight Testing of the X-45A J-UCAS Computational Alpha-Beta System*, AIAA Guidance, Navigation, and Control Conference and Exhibit, Aug, 2006.
- [20] Colgren, R.D., Martin, K.E., *Flight Test Validation of Sideslip Estimation using Inertial Accelerations*, AIAA Guidance, Navigation, and Control Conference and Exhibit, Aug, 2000.
- [21] Setlak, L., and Kowalik, R., *Evaluation of the VSC-HVDC system performance in accordance with the more electric aircraft concept*, 2018 19th International Scientific Conference on Electric Power Engineering, EPE 2018, Proceedings.
- [22] Bjarke, L.J., and Ehernberger, L.J., *An In-Flight Technique for Wind Measurement in Support of the Space Shuttle Program*, NASA TM4154, 1989, pp. 3-4.
- [23] Cho, A., Kim, J., Lee, S., and Kee, C., *Wind Estimation and Airspeed Calibration using a UAV with a Single-Antenna GPS Receiver and Pitot Tube*, IEEE Transactions on aerospace and electronics systems, 47 (2011), pp. 109-115.
- [24] Setlak, L., Kowalik, R., and Redo, W., *Technological solutions of selected components of energo-electronic power supply system PES in the field of AC/DC/DC processing in accordance with a trend of more electric aircraft*, International Journal of Circuits, Systems and Signal Processing, Volume 11, 2017.
- [25] Zeis, J.E., *Angle of Attack and Sideslip Estimation using an Inertial Reference Platform*, AD-A194 876, Jun, 1988.
- [26] Axford, D. N., *On the Accuracy of Wind Measurements Using an Inertial Platform in an Aircraft, and an Example of a Measurement of the Vertical Mesostructure of the Atmosphere*, Journal of Applied Meteorology, 7 (1968), pp. 645-666.
- [27] Heller, M., Myschiky, S., Holzapfelz, F. and Sachsx, G., *Low-Cost Approach Based on Navigation Data For Determining Angles of Attack and Sideslip for Small Aircraft*, AIAA Guidance, Navigation, and Control Conference and Exhibit, Aug, 2003.
- [28] Byeon, G. Y., Park, S., *Backward Path Following under a Strong Headwind for UAV*, J. of The Korean Society for Aeronautical and Space Sciences, 42 (2014), pp. 376-382.
- [29] Phillips, Caleb, Sicker, Douglas, Grunwald, Dirk, *A Survey of Wireless Path Loss Prediction and Coverage Mapping Methods*, Communications Surveys & Tutorials IEEE, vol. 15, no. 1, pp. 255-270, 2013.
- [30] Setlak, L., and Kowalik, R., *Study of the transformer rectifier unit compatible with the concept of a more electric aircraft*, 2018 Progress in Applied Electrical Engineering, PAEE 2018.
- [31] Lee, Yee Hui, Meng Song, Yu, *Impact of sapling movements on VHF and UHF radio-wave propagations*, Antennas and Propagation Society International Symposium (APSURSI) 2013 IEEE, pp. 1620-1621, 2013.